The Astrophysical Journal, 666:967–975, 2007 September 10

THE STRUCTURE OF THE HOMUNCULUS. III. FORMING A DISK AND BIPOLAR LOBES IN A ROTATING SURFACE EXPLOSION[1]

Nathan Smith
Astronomy Department, 601 Campbell Hall, University of California, Berkeley, CA 94720; nathans@astro.berkeley.edu

and

Richard H. D. Townsend
Bartol Research Institute, University of Delaware, Newark, DE 19716; rhdt@batol.udel.edu
Received 2007 February 17; accepted 2007 April 30

ABSTRACT

We present a semianalytic model for the shaping of the Homunculus Nebula around η Carinae that accounts for the simultaneous production of bipolar lobes and an equatorial disk through a rotating surface explosion. Material is launched normal to the surface of an oblate rotating star with an initial kick velocity that scales approximately with the local escape speed. Thereafter, ejecta follow ballistic orbital trajectories, feeling only a central force corresponding to a radiatively reduced gravity. Our model is conceptually similar to the wind-compressed disk model of Bjorkman & Cassinelli, but we modify it to an explosion instead of a steady line-driven wind, we include a rotationally distorted star, and we treat the dynamics somewhat differently. A continuum-driven explosion, where the radiation force is independent of velocity, avoids the disk inhibition mechanisms that normally operate in line-driven winds. This allows midlatitude material with appropriate initial specific energy to migrate toward the equator, where it collides with material from the opposite hemisphere to form a disk. Thus, our model provides a simple method by which rotating hot stars can simultaneously produce intrinsically bipolar and equatorial mass ejections, without relying on an aspherical environment or magnetic fields. Although motivated by η Carinae, the model may have generic application to episodic mass ejection where rotation is important, including other luminous blue variables, B[e] stars, the nebula around SN 1987A, or possibly even bipolar supernova explosions themselves. In cases where near-Eddington radiative driving is less influential, our model generalizes to produce bipolar pinched-waist morphologies without disks, as seen in many planetary nebulae. If rotating single stars can produce strongly axisymmetric ejecta by this mechanism, then the presence of aspherical ejecta by itself is insufficient justification to invoke close binary evolution.

Subject headings: circumstellar matter — ISM: individual (Homunculus Nebula) — stars: individual (η Carinae) — stars: mass loss — stars: rotation — stars: winds, outflows

1. INTRODUCTION

It is commonly assumed that shell nebulae surrounding massive hot stars, such as luminous blue variables (LBVs), consist of slow ambient material that has been swept up by the faster wind of the hot supergiant. This scenario is often adopted to explain the origin of bipolar geometry in their nebulae, by applying the generalized interacting stellar winds (GISW) scenario that was developed successfully for bipolar planetary nebulae and related outflow phenomena (e.g., Mellema et al. 1991; Frank et al. 1996; Balick & Frank 2002), as well as for the famous nebula around SN 1987A (Luo & McCray 1991; Wang & Mazzali 1992; Blondin & Lundqvist 1993; Martin & Arnett 1995). In this scenario, a hot fast wind expands into a slower wind from a previous red supergiant (RSG) or asymptotic giant branch (AGB) phase. The surrounding slow wind must have an equatorial density enhancement (i.e., a disk), and the consequent mass loading near the equator slows the expansion of the shock interface between the two winds, giving rise to a pinched waist and bipolar structure. However, it remains unclear how the required pre-existing disk can be formed. One does not normally expect RSG or AGB stars to be rotating rapidly enough to form an equatorial decretion disk, such as is characteristic of Be stars (Porter & Rivinius 2003), and thus a disk-shedding scenario probably requires the tidal influence of a companion during prior evolutionary phases in order to add sufficient angular momentum. In the case of SN 1987A, a binary merger would be required for this particular scenario to work (Collins et al. 1999). As an alternative, variations of the GISW paradigm can be invoked (e.g., including an aspherical fast wind expanding into a spherical slow wind) to reproduce the bipolar shape of the nebula around η Carinae (Frank et al. 1995, 1998; Dwarkadas & Balick 1998; Langer et al. 1999; Gonzalez et al. 2004a, 2004b).

However, it is unlikely that this general scenario can work for massive LBVs like η Carinae, or for SN 1987A. Stars with luminosities above roughly $10^{5.8}\ L_{\odot}$ never reach the RSG stage, and the coolest apparent temperatures that they can achieve occur instead during the LBV phase.[2] As they evolve off the main sequence, they move to the right on the HR diagram, toward cooler temperatures, larger stellar radii, and lower values for their escape velocities. Consequently, their stellar wind speeds get slower—not faster—as their mass-loss rates increase. O-type

[1] Based in part on observations obtained at the Gemini Observatory, which is operated by AURA, under a cooperative agreement with the NSF on behalf of the Gemini partnership: the National Science Foundation (US), the Particle Physics and Astronomy Research Council (UK), the National Research Council (Canada), CONICYT (Chile), the Australian Research Council (Australia), CNPq (Brazil), and CONICET (Argentina).

[2] Admittedly, there is also a group of relatively low luminosity LBVs around $\log(L/L_{\odot}) = 5.5$ (see Smith et al. 2004a) where the GISW may still apply, because these stars may be in a post-RSG phase.

stars have typical wind speeds of a few 10^3 km s^{-1}, whereas LBVs typically have terminal wind speeds of a few 10^2 km s^{-1} and mass-loss rates a factor of $\sim$100–1000 higher. This creates a situation where a slow dense wind is expanding freely into a faster and much lower density wind, which is *exactly the opposite* situation of that required for the usual GISW scenario to work. In other words, the winds are not strongly interacting.

The specific case of SN 1987A presents its own set of difficulties, even though its progenitor is well below $\log(L/L_\odot) = 5.8$ and it probably has been through a recent RSG phase. First, a merger model followed by a transition from a RSG to BSG requires that these two events be synchronized with the supernova event itself (to within the $\sim 10^4$ yr dynamical age of the nebula), requiring that the best observed supernova in history also happens to be a very rare event. One could easily argue, however, that the merger (needed for the bipolar geometry) and the blue loop scenario might not have been invented if SN 1987A had occurred in a much more distant galaxy where it would not have been so well observed (i.e., we would not know about the bipolar nebula or the BSG progenitor). Second, after the RSG swallowed a companion star and then contracted to become a BSG, it should have been rotating at or near its critical velocity (e.g., Eriguchi et al. 1992). Even though pre-explosion spectra (Walborn et al. 1989) do not have sufficient resolution to measure line profiles, Sk $-69^\circ 202$ showed no evidence of rapid rotation (e.g., like a B[e] star spectrum). Third, and particularly troublesome, is that this merger and RSG/BSG transition *would need to occur twice*. From an analysis of light echoes for up to 16 yr after the supernova, Sugerman et al. (2005) have identified a much larger bipolar nebula with the same axis orientation as the more famous inner triple-ring nebula. If a merger and RSG/BSG transition are to blame for the bipolarity in the triple-ring nebula, then what caused it in the older one? Perhaps a more natural explanation would be that Sk $-69^\circ 202$ suffered a few episodic mass ejections analogous to LBV eruptions in its BSG phase (see Smith 2007). The B[e] star R4 in the Small Magellanic Cloud may offer a precedent at the same luminosity as the progenitor of SN 1987A; R4 is consistent with a 20 $M_\odot$ evolutionary track, and it experienced a minor LBV outburst in the late 1980s (Zickgraf et al. 1996). R4 also has elevated nitrogen abundances comparable to the nebula around SN 1987A.

For η Carinae, observations have falsified the idea that the bipolar shape arises from a prior equatorial density enhancement (Smith 2006). In the GISW scenario, the nebula's waist gets pinched because of mass loading, so in the resulting bipolar nebula there should be an excess of mass at low latitudes compared to a spherical shell. Instead, detailed observations of the latitudinal mass dependence in the Homunculus show that the mass was concentrated toward high polar latitudes (Smith 2006). Furthermore, observations show no evidence for a preexisting slow disk around η Car that could have pinched the waist. Instead, the disk structure that is seen in high-resolution images, usually called the "equatorial skirt," has measured kinematics indicating an origin *at the same time* as the bipolar lobes (Morse et al. 2001). Some material appears to be even *younger*, not older (Smith & Gehrz 1998; Davidson et al. 1997, 2001; Smith et al. 2004b; Dorland et al. 2004). Thus, any model for the production of the bipolar Homunculus also needs to be able, simultaneously, to produce a thin equatorial disk. The only model proposed so far to accomplish this is in the thermally driven magnetic wind model of Matt & Balick (2004) intended for the presently observed bipolar wind (Smith et al. 2003a). However, it is not known if the extreme magnetic field required to shape the massive Homunculus is achievable, because the conditions during the 19th century eruption were much more extreme than in the stellar wind seen now.

If LBV nebulae cannot be dominated by swept up ambient material, we are left in need of an alternative explanation for the origin of their bipolar structure. Several recent clues, due in large part to detailed observations of η Carinae, point instead toward the idea that LBV eruptions can behave more like explosions than steady winds:

1. The ratio of total mechanical energy to radiated energy for the 19th century eruption of η Car was greater than unity, and the ratio of kinetic momentum to photon momentum was $\sim 10^3$ (Smith et al. 2003b). These numbers are characteristic of explosions rather than winds.
2. Most of the mass in the Homunculus is concentrated in a very thin shell seen in H_2 emission (Smith 2006), which implies that Δt for the mass-loss event was $\lesssim$5 yr. Proper motions also suggest a similarly small range of ejection dates (Morse et al. 2001). Ejecting the observed amount of mass in the Homunculus over that short a time requires a mass-loss rate of order 1 $M_\odot$ yr^{-1} or higher (Smith et al. 2003b; Smith 2006), which may surpass the capability of even a super-Eddington continuum-driven wind by itself (Owocki et al. 2004).
3. The high polar expansion speed in the Homunculus (about 650 km s^{-1}) is close to the expected escape velocity of the primary star, ignoring radiation pressure. In a radiatively driven stellar wind, one expects the speed to drop as a star nears the Eddington limit, because of the lower effective gravity. However, in an optically thick hydrodynamic explosion that is not initially driven by radiation force, this condition would not necessarily apply.

In this paper, we examine the idea that a surface explosion from a rapidly rotating hot star can create an intrinsically bipolar nebula and thin disk, without relying on any latitude dependence in the ambient material, binary influence, or magnetic fields. Thus, our model adopts the simplest set of assumptions that are also physically plausible.

2. THE MODEL: A ROTATING SURFACE EXPLOSION

2.1. *Basic Principles*

Our simple model traces its origins back to a key question concerning the morphology of η Car's Homunculus: can a single basic physical paradigm account for the simultaneous production of both the equatorial skirt and the bipolar lobes? In considering this question, the phenomenon of rotation naturally springs to mind, since material kicked ballistically from the surface of a rotating star has a natural tendency to migrate toward the stellar equatorial plane. This notion was invoked in the wind-compressed disk (WCD) model of Bjorkman & Cassinelli (1992, 1993) as a means of explaining the circumstellar disks around Be stars. The WCD model treats the wind plasma as independent fluid parcels whose dynamics are confined to their respective orbital planes. Detailed calculations by Owocki et al. (1998) demonstrated that subtle line-driving effects associated with velocity-dependent forces tend to inhibit the formation of disks in the WCD model. However, in our treatment below, we focus on continuum driving, which is independent of velocity, and the WCD model furnishes a useful paradigm on which to build.

We advance the hypothesis that, to first order, the shape of the Homunculus can be understood as the consequence of the nearly ballistic, anisotropic ejection of the surface layers of a star near its critical rotation limit. In this scenario, the bipolar shape and

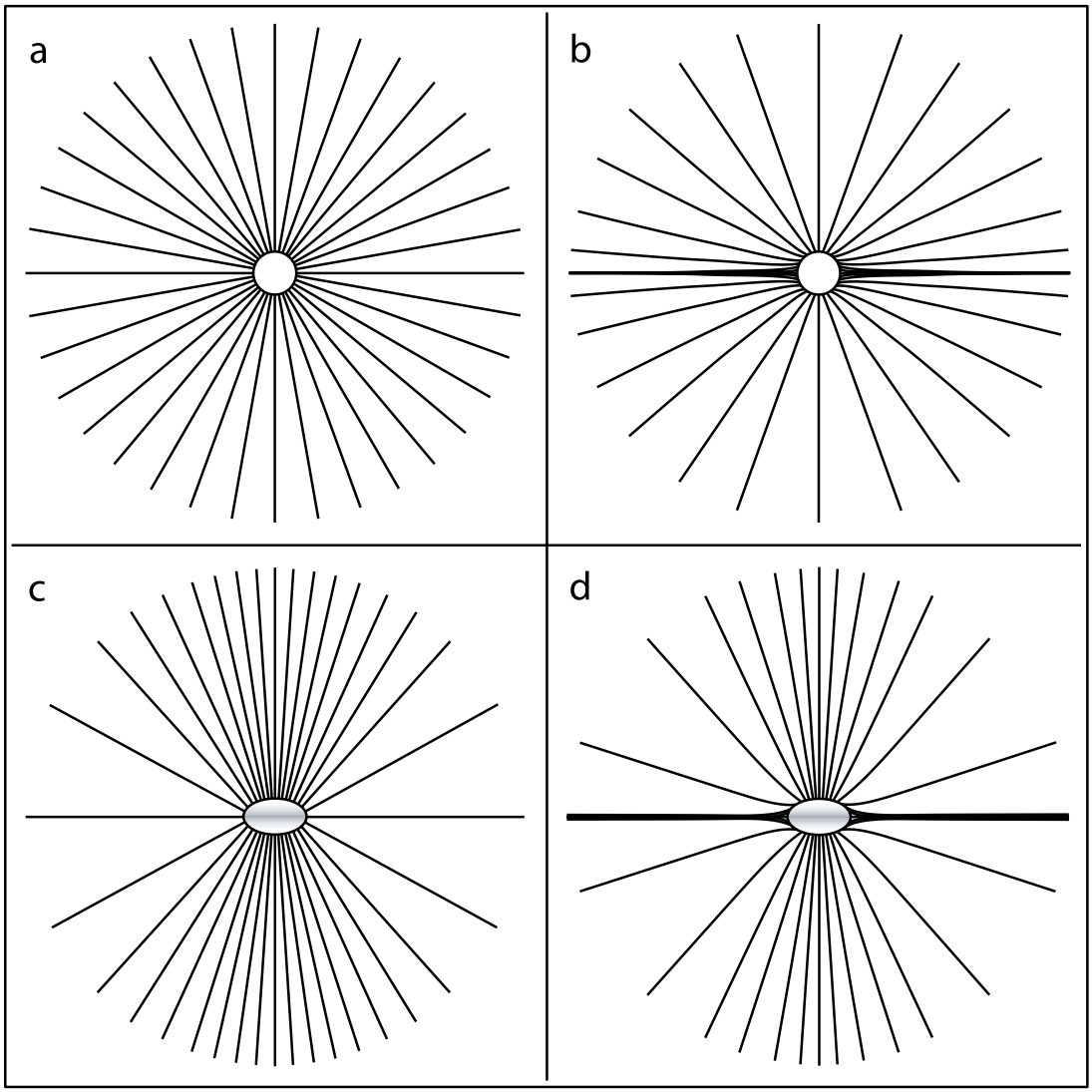

FIG. 1.—Simple conceptual sketch of the various levels of complexity for trajectories in a rotating explosion. (*a*) Purely radial trajectories from a spherical nonrotating star. (*b*) Orbital trajectories from a spherical rotating star, where material is diverted toward the equator, as in the wind compressed disk model of Bjorkman & Cassinelli (1993). (*c*) Same as (*a*), but with ejection normal to the surface of an oblate star. (*d*) A combination of (*b*) and (*c*), where material is ejected normal to the surface of an oblate star, but where rotation modifies the trajectories. This still enhances the polar density, but rapid rotation also diverts material toward the equator to form a compressed disk. The shading in (*c*) and (*d*) is to remind us of equatorial gravity darkening.

equatorial disk arise as a direct consequence of the ejection geometry, rather than through hydrodynamic interaction afterward. We assume that the subsequent evolution of these layers is governed solely by a central, gravity-like ($1/r^2$) force, and therefore that the trajectory followed by each fluid element may be treated as a problem in orbital dynamics. The exception is for elements that pass through the equatorial plane; there, we assume that they collide with material from the opposite hemisphere, leading to the cancellation of their velocity component normal to the plane. We ignore the self-gravity of the ejected mass.

Sketches of the trajectories for outflowing material under various levels of complexity are illustrated in Figure 1. These trajectories show in principle how density can be enhanced at the equator to form a disk, as well as toward the poles. When a spherical star with radial trajectories (Fig. 1*a*) is allowed to rotate rapidly, material is diverted toward the equator (Fig. 1*b*) by conservation of angular momentum, as envisioned in the WCD model. However, a severely oblate star introduces other effects as well. First, as noted above, an oblate star has a smaller radius, larger effective gravity, and larger escape velocity at the pole than at the equator. This, rather than the latitude dependence of density, is what gives rise to the bipolar *shape* of the nebula. The oblateness of the star will also enhance the polar *density* if material is initially launched normal to the surface, simply because the flatter poles of the star aim trajectories poleward (Fig. 1*c*). We do not attempt to model this enhanced polar density quantitatively, however, because we expect that additional effects may be as important. For example, the polar mass flux can be increased by the stronger radiative flux at the poles of a star that suffers from rotationally induced gravity darkening (e.g., Owocki & Gayley 1997; Owocki et al. 1998). In any case, the straight (i.e., nonrotating) trajectories from a rotationally distorted star in Figure 1*c* seem unrealistic unless the ejecta speeds are much faster than the rotation speed. The more likely rotationally modified trajectories are shown conceptually in Figure 1*d*. This last case creates a compressed disk, but also retains some degree of enhanced density at the poles, because the rotational wind compression effects are more important at larger cylindrical radii.

Elaborating on this sketch, we consider a model star in an initial state of critical rotation. (We have no direct evidence that

η Car was rotating critically prior to the Great Eruption; however, since the investigation of rotational effects is central to our study, it is appropriate to focus on the critical limit in which these effects are the most pronounced.) In the Roche approximation (e.g., Cranmer 1996, and references therein), the surface radius of the oblate star is given by

$$R(\theta) = \begin{cases} 3\dfrac{\sin(\theta/3)}{\sin\theta} R_p & \text{for } \theta < \pi/2 \\ R(\pi - \theta) & \text{for } \theta > \pi/2 \end{cases} \quad (1)$$

where θ is the usual polar coordinate, and R_p is the polar radius of the star. The azimuthal velocity due to rotation is given by

$$V_\phi(\theta) = \Omega_c R(\theta) \sin\theta, \quad (2)$$

where

$$\Omega_c \equiv \sqrt{\frac{8GM}{27R_p^3}} \quad (3)$$

is the critical angular frequency of rotation in the same Roche approximation, with M the stellar mass and G the gravitational constant.

At $t = 0$, we disrupt this initial state by (1) imparting a velocity kick $V_k(\theta)$ to each surface fluid element in the direction of the local surface normal (this is the *explosion*), and (2) introducing a spherically symmetric force that everywhere is directed radially outward, and whose magnitude is α times the gravitational force. (It is assumed that $\alpha < 1$, so that the *net* force on elements remains directed inward toward the star). This disruption represents our basic characterization of the Great Eruption observed in the 1840s, when the nebular material is thought to have been launched (Morse et al. 2001; Smith & Gehrz 1998; Currie et al. 1996; Gehrz & Ney 1972; Ringuelet 1958; Gaviola 1950). For simplicity, we assume instantaneous ejection rather than sustained outflow over 10–20 yr, but this should have little effect on the overall results. A series of bursts over a decade, as opposed to one single burst, would produce a nebula with a similar shape but some finite thickness.

Our motivation for including the kick (1) and the subsequent outward force (2) comes from considering the effects of continuum radiation driving during the sudden, factor $\sim$5 increase in luminosity associated with the Great Eruption (see, e.g., Davidson & Humphreys 1997). At the beginning of the eruption, rotation-induced gravity darkening will produce a strongly anisotropic radiation field (e.g., von Zeipel 1924; Cranmer & Owocki 1995; Owocki et al. 1996, 1998; Owocki & Gayley 1997; Langer 1998; Glatzel 1998; Maeder 1999; Maeder & Desjacques 2001). This means that the additional radiative flux escaping the star will at first deposit momentum preferentially at the stellar poles; by assuming an appropriate form for $V_k(\theta)$ (discussed in greater detail in the following sections), we use the velocity kick (1) to model this initial polar deposition. As the surface fluid elements subsequently move outward, however, the anisotropies in the radiative flux will tend to be smeared out, leading to a more spherically symmetric outward radiative force that we incorporate via (2).

To determine the $t > 0$ evolution of the surface fluid elements, we assume that each follows a trajectory described by the equation of motion

$$\frac{d\boldsymbol{v}}{dt} = -\frac{GM}{r^3}\boldsymbol{r} + \alpha\frac{GM}{r^3}\boldsymbol{r}. \quad (4)$$

Here, $\boldsymbol{r}$ is the position vector of the element, $\boldsymbol{v} \equiv d\boldsymbol{r}/dt$ is the corresponding velocity vector, and we adopt the convention that nonbold symbols denote the modulus of their bold vector equivalents, so that in this case $r \equiv |\boldsymbol{r}|$. The acceleration terms on the right-hand side of this equation arise, respectively, from the inward gravitational force and the outward spherically symmetric force introduced at $t = 0$. Following the discussion given above, the initial velocity of each element is calculated as

$$\boldsymbol{v}_0 = V_k(\theta)\boldsymbol{e}_n + V_\phi(\theta)\boldsymbol{e}_\phi, \quad (5)$$

where

$$\boldsymbol{e}_n = \frac{\boldsymbol{e}_r - (\boldsymbol{R}'/R)\boldsymbol{e}_\theta}{\sqrt{1 + (R'/R)^2}} \quad (6)$$

is the unit surface normal vector, with $R' \equiv \partial R/\partial\theta$, and $\{\boldsymbol{e}_r, \boldsymbol{e}_\theta, \boldsymbol{e}_\phi\}$ are the unit basis vectors in the spherical-polar $\{r, \theta, \phi\}$ directions.

The equation of motion (eq. [4]) is identical to that for a test particle moving in the gravitational field of a point mass $M(1 - \alpha) > 0$. Therefore, the solutions are analytical, taking the form of conic sections (ellipses, hyperbolae, etc.) whose focus lies at the stellar origin. We leave a detailed discussion of these solutions to any of the many standard texts discussing this classical two-body problem (e.g., Boccaletti & Pucacco 1996). However, it is appropriate to specify how the six orbital parameters, defining the trajectory followed by each surface fluid element, are determined from the initial conditions. First, we calculate the specific (per unit mass) angular momentum vector

$$\boldsymbol{j} = \boldsymbol{r}_0 \times \boldsymbol{v}_0 \quad (7)$$

(where $\boldsymbol{r}_0$ is the element's position at $t = 0$, and $\boldsymbol{v}_0$ was defined in eq. [5]), and the specific Laplace-Runge-Lenz vector

$$\boldsymbol{A} = \boldsymbol{v} \times \boldsymbol{j} - GM(1 - \alpha)\boldsymbol{e}_r. \quad (8)$$

We assume that the reference plane is the stellar equatorial (Cartesian x-y) plane, with the x-axis defining the vernal point. Then, the inclination i of the orbital plane is given by

$$\cos i = \frac{\boldsymbol{j} \cdot \boldsymbol{e}_z}{j}; \quad (9)$$

the longitude of the ascending node Ω and argument of periastron ω by

$$\tan\Omega = \frac{\boldsymbol{e}_z \cdot [\boldsymbol{e}_x \times (\boldsymbol{e}_z \times \boldsymbol{j})]}{\boldsymbol{e}_x \cdot (\boldsymbol{e}_z \times \boldsymbol{j})},$$
$$\tan\omega = \frac{\boldsymbol{j} \cdot [\boldsymbol{A} \times (\boldsymbol{e}_z \times \boldsymbol{j})]}{j\boldsymbol{A} \cdot (\boldsymbol{e}_z \times \boldsymbol{j})}; \quad (10)$$

and the eccentricity e and semimajor axis a by

$$e = \frac{A}{GM(1 - \alpha)}, \qquad a = \left|\frac{GM(1 - \alpha)}{v^2 - 2GM(1 - \alpha)/r}\right|. \quad (11)$$

(In these expressions, $\{\boldsymbol{e}_x, \boldsymbol{e}_z\}$ are the unit basis vectors in the Cartesian$\{x, z\}$ directions.) Finally, the true anomaly υ_0 of the surface element at the $t = 0$ epoch is given by

$$\tan\upsilon_0 = \frac{\boldsymbol{j} \cdot (\boldsymbol{A} \times \boldsymbol{r}_0)}{j\boldsymbol{A} \cdot \boldsymbol{r}_0}. \quad (12)$$

The orbital parameters $\{i, \Omega, \omega, e, a, \upsilon_0\}$ defined above allow calculation of the complete $t > 0$ evolution of a given surface element. However, for those elements whose trajectories pass through the equatorial plane, the parameters must be modified to account for the anticipated collision with material from the opposite hemisphere. As discussed above, the polar (θ) component of the velocity $\boldsymbol{v}$ is set to zero when the element reaches the equator. Then, the orbital parameters are recalculated using the element's instantaneous position and updated velocity, and its evolution is continued.

This approach is rather different from the WCD model of Bjorkman & Cassinelli (1993), who assumed that velocity vectors become radial at the equator, with no change in speed. In fact, a more fundamental difference between our approach and the WCD model lies in the treatment of the outward force introduced at $t = 0$. Bjorkman & Cassinelli (1993) incorporated a parameterization of line-driven wind theory in their model, resulting in an outward radiative force that (1) exceeds gravity and (2) does not have a simple $1/r^2$ scaling. The significance of (1) is that an initial kick (as assumed in our treatment) is not required for material at the stellar poles to escape from the star. However, (2) means that the equation of motion does not correspond to a two-body gravitational problem, and must be integrated numerically.

2.2. *Illustrative Simulations*

To furnish an initial demonstration of our approach, we consider the case where the velocity kick function is given by

$$V_k(\theta) = V_{k,0}|\cos\theta| \tag{13}$$

for some normalizing velocity $V_{k,0}$ at the poles, which in the case of η Car is about 650 km s^{-1} (Smith 2006). The dependence on $|\cos\theta|$ may seem ad hoc in our simulation, because it essentially prescribes the overall shape that is observed. However, this latitude dependence for the initial kick has a firm physical justification. As we discussed above, gravity darkening—whereby the local emergent flux scales with the local effective gravity—tends to initially focus the additional radiative flux escaping from the star toward the stellar poles. Thus, the kick imparted by this flux is expected to be strongest over the poles, suggesting the above form for $V_k(\theta)$.

We should mention that a prescription similar to equation (13) above has already been invoked to explain the bipolar shape of the Homunculus Nebula and the latitude dependence of η Car's stellar wind for near-critical rotation (Owocki 2005; see also Owocki & Gayley 1997; Maeder & Desjacques 2001; Dwarkadas & Owocki 2002; Smith 2002, 2006; Smith et al. 2003a). However, the focus in most of these studies is on the terminal velocity v_∞ of a line-driven wind, whereas in the present study, we are considering the initial kick velocity of an explosive ejection. The reason why a $\cos\theta$ variation is appropriate in the line-driven case is that v_∞ typically scales with the local escape velocity $v_{\rm esc}$ (see, e.g., Dwarkadas & Owocki 2002). Then, with $v_{\rm esc}$ itself scaling with effective gravity in the same way as the radiative flux, a coincidence between V_k and the line-driven v_∞ naturally arises.

For a selected region of the α-$V_{k,0}$ parameter space, we conducted simulations where we evolve a set of surface elements to the asymptotic limit $t \rightarrow \infty$. For each simulation, the initial state at $t = 0$ is comprised of 5000 elements distributed uniformly in θ over the Roche surface described by equation (1). With initial velocities described by equations (2), (5), and (13), these elements are evolved according to the equation of motion (eq. [4]), as described in the preceding section. In the limit of large t, the envelope $R_E(\theta)$ defined by the elements reaches a steady state that corresponds to the eventual shape of the ejected nebula.

Figure 2 compares simulated envelopes $R_E(\theta)$ against the shape of the η Car Homunculus, as measured by Smith (2006). Clearly, with an appropriate choice of parameters—in this case, $\alpha = 0.6$ and $V_{k,0} = 1.5(GM/R_p)^{1/2}$—we are able to capture the gross qualitative features of the bipolar nebula, while at the same time producing the desired equatorial skirt. Generally, a skirt occurs whenever the initial specific energy of surface elements,

$$E_0 = |\boldsymbol{v}_0|^2/2 - GM(1-\alpha)/r_0, \tag{14}$$

exhibits a minimum at some point between equator and pole. (Such minima themselves arise because the kick kinetic energy decreases toward the equator, while the rotational kinetic energy and gravitational potential energy both increase toward the equator.) The surface elements situated at the energy minimum lead to the narrow waist of the envelope. The elements closer to the equator, with higher E_0 and hence faster terminal velocities $v_\infty \propto \sqrt{E_0}$, then form the skirt, while the elements closer to the poles produce the bipolar lobes. In Figure 3, we plot both E_0 and $\sqrt{E_0}$ as a function of θ for the $\alpha = 0.6$, $V_{k,0} = 1.5(GM/R_p)^{1/2}$ simulation. The specific energy minima that give rise to the skirt in this case can clearly be seen at $\theta \approx 80^\circ$ and $\theta \approx 100^\circ$. Note that the tendency of elements to evolve toward the equatorial plane, due to conservation of angular momentum, produces a rather narrower skirt than might be assumed from a cursory look at the plot; compare, for instance, the $\sqrt{E_0}$ data shown in Figure 3 with the center panel of Figure 2. Figure 3 reproduces the trend of higher kinetic energy in the polar ejecta observed in the Homunculus (Smith 2006).

Toward smaller values of α and/or $V_{k,0}$, the initial specific energy of surface elements near the equator is negative. These elements therefore remain gravitationally bound to the star, producing a collapsed-waist morphology with no skirt. The implication is that when generalized to cases where near-Eddington radiative driving is less influential ($\alpha \lesssim 0.5$ in Fig. 2), our model simplifies and easily accommodates the more common pinched-waist morphologies of planetary nebulae without fast skirts (e.g., Balick & Frank 2002). This is encouraging, since these sources have central stars that are indeed far less luminous than η Carinae. Conversely, toward larger α the elements have insufficient angular momentum to reach the equatorial plane, and the skirt is replaced by a local inversion of the bipolar shape. This range of conditions may explain why equatorial disks like that around η Car are not always seen, while bipolar ejecta nebulae are quite common around evolved rotating stars.

2.3. *A Tuned Simulation*

A notable discrepancy between observations and our "best" simulation shown in Figure 2 (*center panel*) is that the apparent flattening of the nebula lobes over the poles is not properly reproduced. This can be seen as faster expansion in the Homunculus at latitudes about 15°–40° from the polar axis, as compared to our predicted shape. It is as if the Homunculus has received an extra kick at these latitudes.

What $V_k(\theta)$ must be adopted in order to reproduce correctly the lobe shapes? One possible answer to this question is presented in Figure 4. Here, the kick velocity function has been tuned with the specific purpose of reproducing the lobe shapes. The tuning was accomplished through a simple process of trial and error,

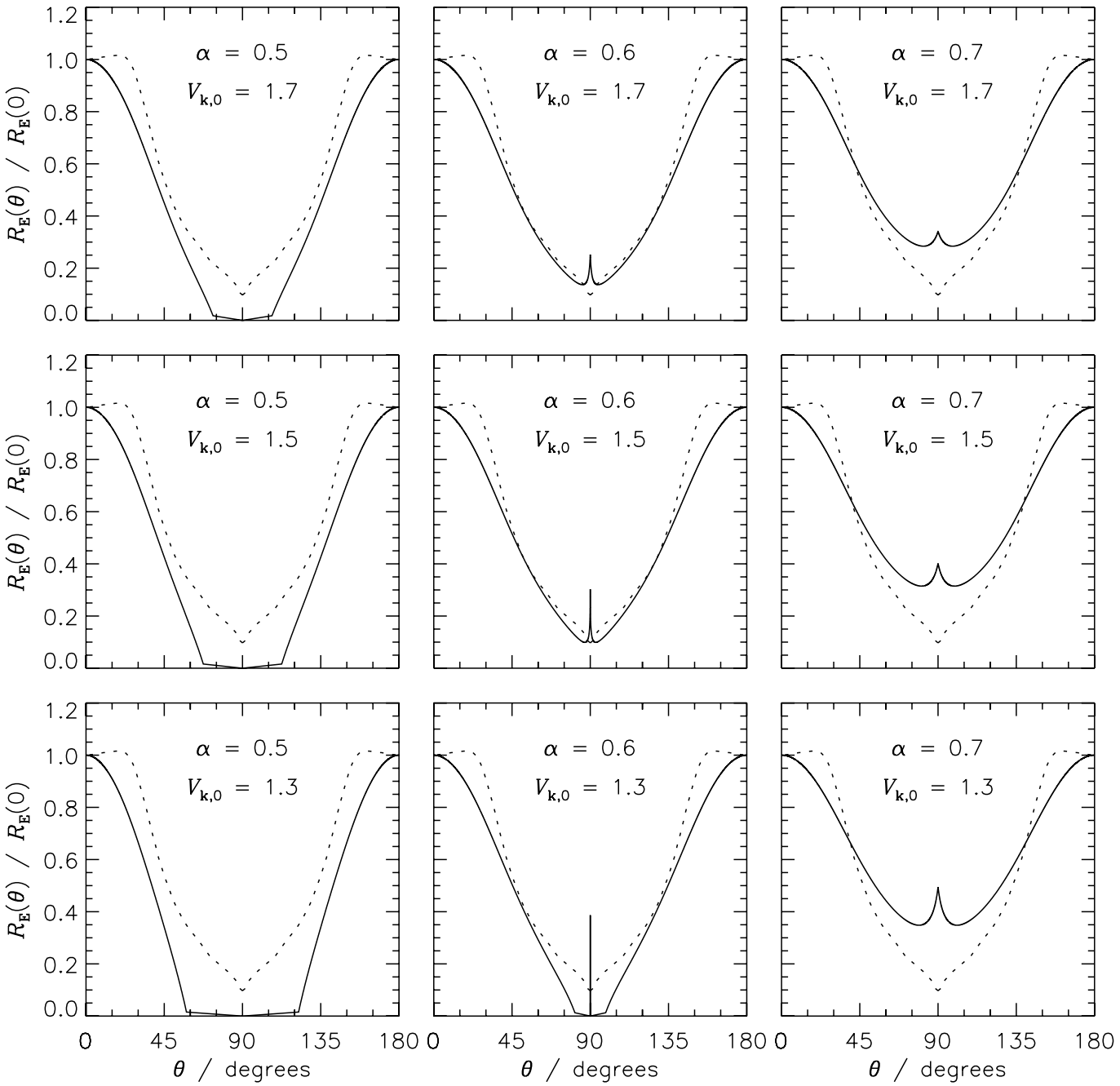

FIG. 2.—Envelopes $R_E(\theta)$ of the ejected surface elements in the asymptotic limit $t \rightarrow \infty$ (*solid line*), plotted together with the measured shape of the Homunculus (*dotted line*) from Smith (2006). Each panel shows results from a simulation with the indicated gravity reduction parameter α and velocity kick normalization $V_{k,0}$, the latter being measured in units of $(GM/R_p)^{1/2}$.

subject to the constraints that $\alpha = 0.6$ and that over the stellar poles $V_k = 1.5(GM/R_p)^{1/2}$ (these values come from the "best" simulation of the preceding section). The close match between theory and observations seen in the central panel of Figure 4 should not be taken as a measure of the fidelity of our model—indeed, since we have adopted an ad hoc prescription for $V_k(\theta)$, the close agreement is to be expected.

However, what *is* of particular significance is the fact that the simulation simultaneously reproduced the lobes *and* a skirt that is similar to that which is actually seen around η Car (e.g., Duschl et al. 1995). Namely, this is a true flattened disklike structure, with material of the same age spread out over a range of radii in the equatorial plane—it is not a ring, even though we adopted an instantaneous explosion event (it is also kinematically different from a Keplerian disk). This is a true success of our model, since the signature of this skirt is wholly absent from the initial kick velocity function in the left panel of Figure 3.

Furthermore, the small extra kick needed at latitudes about 15°–40° from the polar axis may have a reasonable physical explanation. Although our model attributes the overall shape of the Homunculus and its disk to initial conditions of the ejection, this is a case where hydrodynamic shaping of the ejecta long after ejection may play some role after all. We have argued that the GISW scenario cannot drive the overall shape of the Homunculus, largely because the posteruption wind is not powerful enough (Smith 2006; Smith et al. 2003a, 2003b). However,

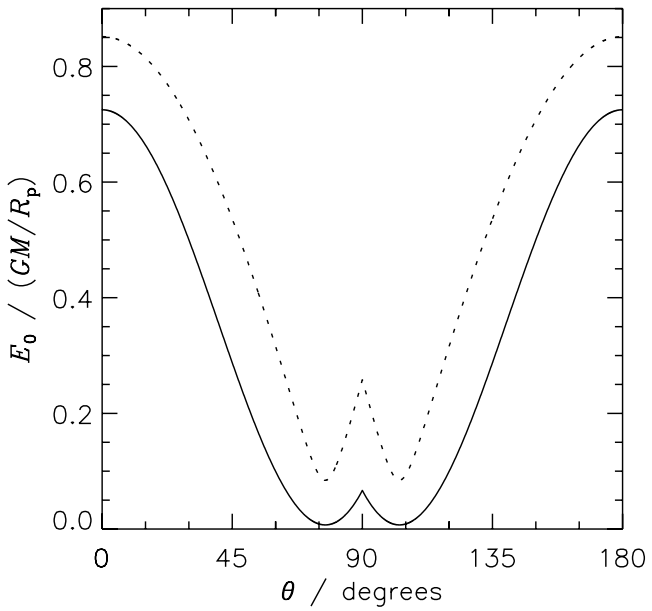

FIG. 3.—Initial specific (per unit mass) energy E_0 (*solid line*) and its square root $\sqrt{E_0}$ (*dotted line*), plotted as a function of θ for the $\alpha = 0.6$, $V_{k,0} = 1.5$ simulation displayed in Fig. 2.

the posteruption wind may be able to modify or perturb the existing shape. It is often seen in hydrodynamic simulations of interacting winds that bipolar nebulae develop "corners" at the outer parts of the polar lobes, leading to flattening over the poles that is reminiscent of the extra velocity we require here (e.g., Cunningham et al. 2005; Frank et al. 1998; Dwarkadas & Balick 1998). This effect arises in the following way: at low latitudes within, say, 45° of the equator, the fast wind that is inflating the bipolar nebula strikes the inner side walls of the dense polar lobes at an oblique angle and is then deflected poleward. This material skims along the inner side walls of the polar lobes and piles up in the corners (see Cunningham et al. 2005), adding an extra kick over a small range of latitudes. Although the average momentum of η Car's posteruption wind is tiny compared to the momentum of the nebula (Smith et al. 2003b), in this scenario, the momentum from a relatively large volume fraction of the posteruption wind is focused on only a small portion of the nebula. This effect is purely hydrodynamic, so our ad hoc approach in Figure 3 may not be the best way to explore it. A better (but computationally more intense) way might be to take our predicted model shape in the central panel of Figure 2 and allow it to be "inflated" and shaped self-consistently by a posteruption wind.

The potential role of the posteruption stellar wind (which is a line-driven wind) that follows the continuum-driven outburst also suggests an interesting "double whammy" for enhancing the bipolar shapes of LBV nebulae. Specifically, Owocki and collaborators (Owocki & Gayley 1997; Owocki et al. 1996, 1998) have demonstrated that radiative line driving not only inhibits the initial formation of an equatorial disk, but also enhances the wind mass-loss rate toward the stellar poles. In the case of η Car, this polar wind has been observed (Smith et al. 2003a). Such a polar wind may enhance the bipolar shape of the initial ejection.

Of course, one can imagine other factors that may modify the shape of the polar lobes in the required way, such as the influence of a nearby companion star. This realm of shaping mechanisms is beyond the scope of our present study, but should be explored further.

3. DISCUSSION

Using a semianalytic model, we have shown that a surface explosion from an oblate star near critical rotation can simultaneously produce an equatorial disk and a pair of polar lobes that closely approximate the observed shape of the Homunculus Nebula around η Carinae. This model is arguably the simplest model that also includes realistic assumptions. It does not require any effects of hydrodynamically interacting winds or magnetic fields to produce the asymmetry. This shows that rotating hot stars can eject intrinsically bipolar nebulae simultaneously with equatorial disks.

Our techniques combine two aspects of theories developed initially for nonspherical line-driven stellar winds, but we modify them to the scenario of a sudden explosion. Namely, our model borrows conceptually from the WCD model of Bjorkman & Cassinelli (1993), as well as the expectation that the ejection speed is proportional to the latitudinal variation of the escape speed on the surface of a rotating star, as noted by several investigators. By adapting these ideas to an explosion with continuum driving, however, our model does not suffer from the

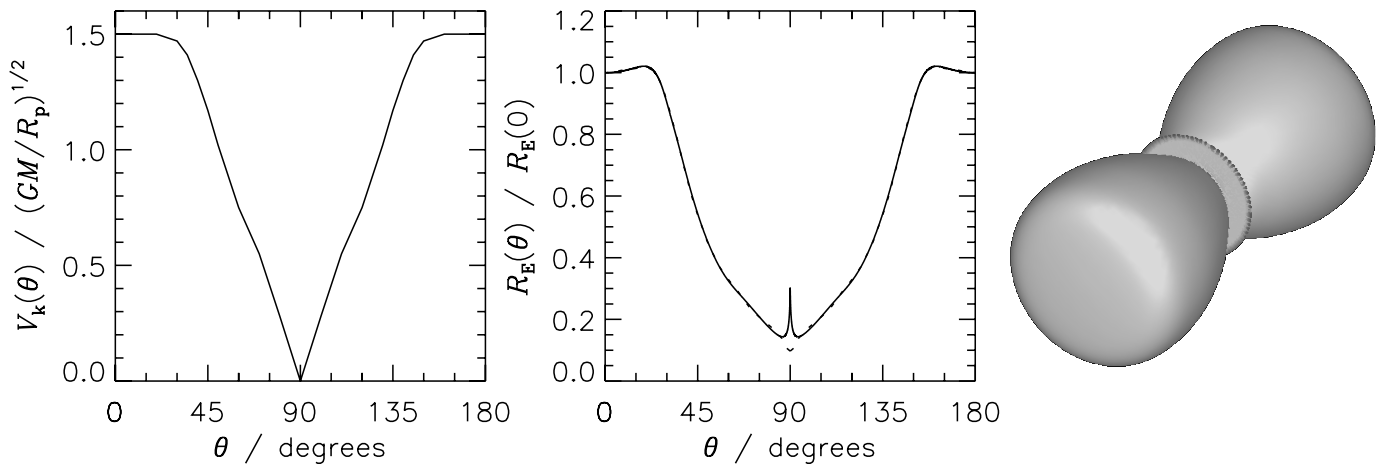

FIG. 4.—Initial kick velocity function (*left panel*), in units of $(GM/R_p)^{1/2}$, tuned to reproduce the shape of the Homunculus (*center panel*; solid and dotted lines have the same meaning as in Fig. 2). A three-dimensional rendering of the corresponding surface of revolution is shown in the right panel; the inclination ($i = 41°$) and orientation (P.A. = 310°) of the surface are based on the values published by Smith (2006).

difficult problem of WCD inhibition due to effects associated with nonradial forces in line-driven winds (Owocki et al. 1998). Whether or not our model is applicable depends on the nature of the episodic mass-loss event in any individual case; the mass loss must be strong enough that it is not dominated by a line-driven wind during an outburst (see Smith & Owocki 2006; Owocki et al. 2004).

Previous models that attempt to explain the shapes of bipolar nebulae around η Carinae and other LBVs differ substantially from ours. Most approaches have used hydrodynamic simulations of interacting winds, where a fast wind sweeps into an equatorial density enhancement to produce the bipolar shape, or variations of that scenario (Frank et al. 1995, 1998; Dwarkadas & Balick 1998; Langer et al. 1999; Gonzalez et al. 2004a, 2004b). However, none of these produced an equatorial disk with the same apparent age as the polar lobes. Soker (2004, and references therein) has discussed a complex model in which accretion onto a companion star drives jets that shape the bipolar lobes, much as in similar models for planetary nebulae, but this model also fails to account for the equatorial disk. Other approaches involving nonspherical stellar winds are closer to our own, where the bipolar shape is an intrinsic feature of ejection from a rotating star (Owocki 2003, 2005; Owocki & Gayley 1997; Dwarkadas & Owocki 2002; Maeder & Desjacques 2001). In these models, the shape of the Homunculus is achieved by such a wind blowing with an enhanced mass-loss rate for a short time. Once again, however, none of these produced an equatorial disk.[3]

One model that did simultaneously produce bipolar lobes and a disk was the thermally driven magnetohydrodynamic rotating stellar wind model of Matt & Balick (2004). While that model was encouraging, we felt it was also useful to pursue alternatives that did not rely on strong magnetic fields, since it is unclear whether the huge fields required to shape the 10–15 $M_{\odot}$ (Smith et al. 2003b) ejected during the Great Eruption are achievable.

Two main assumptions required to produce the observed shape are explosive mass loss with continuum radiative driving and near-critical rotation. Explosive mass loss is justified by the observed fact that η Car lost a huge amount of mass in a short time, with a required mass-loss rate that is too high to be accounted for with a line-driven wind, as noted earlier. Some recent stellar evolution models for very massive stars (Arnett et al. 2005; Young 2005) predict deep-seated hydrodynamic explosions that can potentially release the required amount of kinetic energy of almost 10^{50} ergs seen in the Homunculus (Smith et al. 2003b). Near-critical rotation is expected to occur at late evolutionary stages as a BSG (e.g., Langer et al. 1999; Eriguchi et al. 1992). Soker (2004) has criticized single-star models for the ejection and shaping of the Homunculus, based on the idea that the star spun down during the eruption and was not rotating sufficiently rapidly. However, two points of clarification should be mentioned in this regard. First, near the classical Eddington limit, a star can be near critical rotation for mass loss without necessarily being a true rapid rotator, because of the effects of radiation pressure. Second, while the star may have shed angular momentum by ejecting the Homunculus and therefore was rotating more slowly after the outburst, it is the *initial* rotation and available angular momentum at the time of ejection that is critical, not the end state, especially in an explosion scenario such as that we are discussing here.

The simultaneous formation of a disk and bipolar lobes from the same mechanism is a novel feature of our model, and there are interesting implications for the observed structures. The equatorial ejecta of η Carinae were originally described as a "skirt" rather than a "disk," because of their ragged, streaked appearance, which is different from the clumpy character of the polar lobes (e.g., Morse et al. 1998; Duschl et al. 1995; Zethson et al. 1999). This expanding excretion structure should not be confused with a Keplerian disk. In our proposed scenario for the formation of η Car's skirt, material ejected from midlatitudes on the star migrates toward the equatorial plane, where it crashes into material from the opposite hemisphere. One can easily envision a violent collision that could lead to the ragged spray of ejecta seen today, rather than a smooth disk, and hydrodynamic simulations of this would be interesting. It seems likely that this violent splashing at the equatorial plane could create even faster disk material than the speeds seen in our simulations, where we simply canceled out the vertical component of the velocity. To be sure, there are additional complexities in η Car's equatorial ejecta that we do not even attempt to treat here. Most notable among them are the origin of the NN jet (Meaburn et al. 1993; Walborn & Blanco 1988) and the presence of younger ejecta from the 1890 eruption that appear to coexist with older ejecta in the skirt (Smith & Gehrz 1998; Davidson et al. 2001; Smith et al. 2004b).

Finally, we expect that our proposed scenario could have wider applications beyond the Homunculus around η Carinae. A simple mechanism for how a rotating hot star can simultaneously produce equatorial and polar ejecta might be relevant for the famous triple-ring nebula around SN 1987A (Burrows et al. 1995), providing a possible way to circumvent difficulties in explaining this object via the GISW scenario (see Smith 2007). Likewise, it may apply to bipolar ejecta and rings around other blue supergiants in our Galaxy, such as Sher 25 (Brandner et al. 1997) and the LBV candidate HD 168625 (Smith 2007), as well as LBVs in general. If extragalactic analogs of η Carinae behave similarly in their outbursts, then one might expect the so-called "supernova impostors" to be significantly polarized. The mechanism may also be applicable to the short lived emitting disks around B[e] stars (Zickgraf et al. 1986, 1996) or possibly other hot stars where episodic mass ejection is important.

An encouraging property of our model is that in cases where near-Eddington radiative driving is less influential than in η Carinae (such as in lower luminosity planetary nebulae), the mechanism proposed here generalizes to a situation that reproduces a simple bipolar pinched-waist morphology without an obvious fast disk. Thus, scenarios like those in the left column of Figure 2 may have wide application to observed morphologies of bipolar planetary nebulae, which generally lack such disks (Balick & Frank 2002).

Some supernova explosions are seen to be intrinsically asymmetric; the bipolar supernova ejecta in SN 1987A are seen directly (Wang et al. 2002), while others show polarization at early times (e.g., Leonard et al. 2000, 2001; Leonard & Filippenko 2001). If near-critical rotation is important at some point within these explosions, it is conceivable that our model described here may offer an alternative to jet-driven hydrodynamic models for explaining some aspects of asymmetric core-collapse supernovae.

In any case, a viable mechanism for a single star to produce strongly axisymmetric ejecta means that the presence of asymmetry in the circumstellar environment is, by itself, not a valid

[3] Maeder & Desjacques (2001) presented a second case where a steady stellar wind included a dense disk. However, while this model may account for the enhanced density at the equator, it does not account for the shape (i.e., the speed) that can produce a disk at the same time as the polar lobes. It also depends on effects in line-driven winds that are not applicable to the Great Eruption of η Carinae that produced the Homunculus; S. Owocki (2007, private communication) has noted the difficulty in forming disks via this type of opacity mechanism in radiatively driven winds.

justification to invoke close binary interactions in a supernova progenitor or any other hot massive star.

We gratefully acknowledge many fruitful discussions and collaborations with Stan Owocki, which have shaped our view and aided our understanding of nonspherical mass loss, and we thank an anonymous referee for constructive comments. N. S. was partially supported by NASA through grant HF-01166.01A from the Space Telescope Science Institute, which is operated by the Association of Universities for Research in Astronomy, Inc., under NASA contract NAS5-26555. R. H. D. T. was supported by NASA grant NNG05GC36G. Partial support was provided by NASA through grant GO-10241 from the Space Telescope Science Institute.

REFERENCES

Arnett, D., Meakin, C., & Young, P. A. 2005, in ASP Conf. Ser. 332, The Fate of the Most Massive Stars, ed. R. Humphreys & K. Stanek (San Francisco: ASP), 75
Balick, B., & Frank, A. 2002, ARA&A, 40, 439
Bjorkman, J. F., & Cassinelli, J. P. 1992, in ASP Conf. Ser. 22, Nonisotropic and Variable Outflows from Stars, 88
———. 1993, ApJ, 409, 429
Blondin, J., & Lundqvist, P. 1993, ApJ, 405, 337
Boccaletti, D., & Pucacco, G. 1996, Theory of Orbits (Heidelberg: Springer)
Brandner, W., Grebel, E. K., Chu, Y. H., & Weis, K. 1997, ApJ, 475, L45
Burrows, C. J., et al. 1995, ApJ, 452, 680
Collins, T. J. B., Frank, A., Bjorkman, J. E., & Livio, M. 1999, ApJ, 512, 322
Cranmer, S. R. 1996, Ph.D. thesis, Univ. Delaware
Cranmer, S. R., & Owocki, S. P. 1995, ApJ, 440, 308
Cunningham, A., Frank, A., & Hartmann, L. 2005, ApJ, 631, 1010
Currie, D. G., et al. 1996, AJ, 112, 1115
Davidson, K., & Humphreys, R. M. 1997, ARA&A, 35, 1
Davidson, K., Smith, N., Gull, T. R., Ishibashi, K., & Hillier, D. J. 2001, AJ, 121, 1569
Davidson, K., et al. 1997, AJ, 113, 335
Dorland, B. N., Currie, D. G., & Hajian, A. R. 2004, AJ, 127, 1052
Duschl, W. J., Hofmann, K. H., Rigaut, F., & Weigelt, G. 1995, Rev. Mex. AA Ser. Conf., 2, 17
Dwarkadas, V. V., & Balick, B. 1998, AJ, 116, 829
Dwarkadas, V. V., & Owocki, S. P. 2002, ApJ, 581, 1337
Eriguchi, Y., Yamaoka, H., Nomoto, K., & Hashimoto, M. 1992, ApJ, 392, 243
Frank, A., Balick, B., & Davidson, K. 1995, ApJ, 441, L77
Frank, A., Balick, B., & Livio, M. 1996, ApJ, 471, L53
Frank, A., Ryu, D., & Davidson, K. 1998, ApJ, 500, 291
Gaviola, E. 1950, ApJ, 111, 408
Gehrz, R. D., & Ney, E. P. 1972, S&T, 44, 4
Glatzel, W. 1998, A&A, 339, L5
Gonzalez, R., de Gouveia Dal Pino, E. M., Raga, A. C., & Velazquez, P. F. 2004a, ApJ, 600, L59
———. 2004b, ApJ, 616, 976
Langer, N. 1998, A&A, 329, 551
Langer, N., Garcia-Segura, G., & MacLow, M. M. 1999, ApJ, 520, L49
Leonard, D. C., & Filippenko, A. V. 2001, PASP, 113, 920
Leonard, D. C., Filippenko, A. V., Ardila, D. R., & Brotherton, M. S. 2001, ApJ, 553, 861
Leonard, D. C., Filippenko, A. V., Barth, A. J., & Matheson, T. 2000, ApJ, 536, 239
Luo, D., & McCray, R. 1991, ApJ, 379, 659
Maeder, A. 1999, A&A, 347, 185
Maeder, A., & Desjacques, V. 2001, A&A, 372, L9
Martin, C. L., & Arnett, D. 1995, ApJ, 447, 378
Matt, S., & Balick, B. 2004, ApJ, 615, 921
Meaburn, J., Gehring, G., Walsh, J. R., Palmer, J. W., Lopez, J. A., Bryce, M., & Raga, A. C. 1993, A&A, 276, L21
Mellema, G., Eulderink, F., & Icke, V. 1991, A&A, 252, 718
Morse, J. A., Davidson, K., Bally, J., Ebbets, D., Balick, B., & Frank, A. 1998, AJ, 116, 2443
Morse, J. A., Kellogg, J. R., Bally, J., Davidson, K., Balick, B., & Ebbets, D. 2001, ApJ, 548, L207
Owocki, S. P. 2003, in IAU Symp. 212, A Massive Star Odyssey: From Main Sequence to Supernova, ed. K. van der Hucht, A. Herrero, & C. Esteban (San Francisco: ASP), 281
———. 2005, in ASP Conf. Ser. 332, The Fate of the Most Massive Stars, ed. R. Humphreys & K. Stanek (San Francisco: ASP), 169
Owocki, S. P., Cranmer, S. R., & Gayley, K. G. 1996, ApJ, 472, L115
———. 1998, Ap&SS, 260, 149
Owocki, S. P., & Gayley, K. G. 1997, in ASP Conf. Ser. 120, Luminous Blue Variables: Massive Stars in Transition, ed. A. Nota & H. Lamers (San Francisco: ASP), 121
Owocki, S. P., Gayley, K. G., & Shaviv, N. J. 2004, ApJ, 616, 525
Porter, J. M., & Rivinius, T. 2003, PASP, 115, 1153
Ringuelet, A. E. 1958, Z. Astrophys., 46, 276
Smith, N. 2002, MNRAS, 337, 1252
———. 2006, ApJ, 644, 1151
———. 2007, AJ, 133, 1034
Smith, N., Davidson, K., Gull, T. R., Ishibashi, K., & Hillier, D. J. 2003a, ApJ, 586, 432
Smith, N., & Gehrz, R. D. 1998, AJ, 116, 823
Smith, N., Gehrz, R. D., Hinz, P. M., Hoffmann, W. F., Hora, J. L., Mamajek, E. E., & Meyer, M. R. 2003b, AJ, 125, 1458
Smith, N., & Owocki, S. P. 2006, ApJ, 645, L45
Smith, N., Vink, J., & de Koter, A. 2004a, ApJ, 615, 475
Smith, N., et al. 2004b, ApJ, 605, 405
Soker, N. 2004, ApJ, 612, 1060
Sugerman, B. E. T., Crotts, A. P. S., Kunkel, W. E., Heathcote, S. R., & Lawrence, S. S. 2005, ApJS, 159, 60
von Zeipel, H. 1924, MNRAS, 84, 665
Walborn, N. R., & Blanco, B. M. 1988, PASP, 100, 797
Walborn, N. R., Prevot, M. L., Prevot, L., Wamsteker, W., Gonzalez, R., Gilmozzi, R., & Fitzpatrick, E. L. 1989, A&A, 219, 229
Wang, L., & Mazzali, P. A. 1992, Nature, 355, 58
Wang, L., et al. 2002, ApJ, 579, 671
Young, P. A. 2005, in ASP Conf. Ser. 332, The Fate of the Most Massive Stars, ed. R. Humphreys & K. Stanek (San Francisco: ASP), 190
Zethson, T., Johansson, S., Davidson, K., Humphreys, R. M., Ishibashi, K., & Ebbets, D. 1999, A&A, 344, 211
Zickgraf, F. J., Kovacs, J., Wolf, B., Stahl, O., Kaufer, A., & Appenzeller, I. 1996, A&A, 309, 505
Zickgraf, F. J., Wolf, B., Stahl, O., Leitherer, C., & Appenzeller, I. 1986, A&A, 163, 119